

Revealing Star Formation in the Galactic Center with JWST-NIRCam

Rubén Fedriani¹, Samuel Crowe², Jonathan C. Tan^{3,2}, Alva Kinman³, Yichen Zhang⁴, Morten Andersen⁵, Lucía Bravo Ferres¹, Francisco Nogueras-Lara⁵, Rainer Schödel¹, John Bally⁶, Adam Ginsburg⁷, Yu Cheng⁸, Yao-Lun Yang⁹, Sarah Kendrew¹⁰, Chi-Yan Law¹¹, Joseph Armstrong³, and Zhi-Yun Li²

¹ Instituto de Astrofísica de Andalucía, CSIC, Glorieta de la Astronomía s/n, E-18008 Granada, Spain

² Dept. of Astronomy, University of Virginia, Charlottesville, Virginia 22904, USA

³ Department of Space, Earth & Environment, Chalmers University of Technology, 412 93 Gothenburg, Sweden

⁴ Department of Astronomy, Shanghai Jiao Tong University, 800 Dongchuan Rd., Minhang, Shanghai 200240, China

⁵ European Southern Observatory, Karl-Schwarzschild-Strasse 2, D-85748 Garching bei München, Germany

⁶ Center for Astrophysics and Space Astronomy, Astrophysical and Planetary Sciences Department, University of Colorado, UCB 389 Boulder, CO 80309, USA

⁷ Department of Astronomy, University of Florida, P.O. Box 112055, Gainesville, FL, USA

⁸ National Astronomical Observatory of Japan, 2-21-1 Osawa, Mitaka, Tokyo 181-8588, Japan

⁹ Star and Planet Formation Laboratory, RIKEN Cluster for Pioneering Research, Wako, Saitama 351-0198, Japan

¹⁰ European Space Agency, Space Telescope Science Institute, Baltimore, MD, USA

¹¹ Osservatorio Astrofisico di Arcetri, Largo Enrico Fermi, 5, 50125 Firenze FI, Italy

Abstract

Massive stars are significant throughout the universe, however the mechanism by which they form is poorly understood. Here we present JWST-NIRCam observations of the Galactic Center molecular cloud Sagittarius C (Sgr C) in order to take a census of its star formation activity and test theoretical models of massive star formation in this extreme environment. In conjunction with ancillary NIR, MIR, FIR, and sub-mm data from Spitzer, SOFIA, Herschel, and ALMA, we characterise the massive protostars in G359.44-0.102 via SED fitting obtaining masses of $\sim 20 M_{\odot}$. The NIRCam data reveals in high resolution the outflows from these protostellar sources in the form of atomic and molecular hydrogen shocked material as well as large-scale ionised (HII) gas structures surrounding the main protocluster as traced by Brackett Alpha. Global color analysis also indicates the presence of YSO candidates across the field and helps shed light on the protocluster environment in this extreme region. Finally, we report the discovery of a new star-forming region, named G359.42-0.104, $1'$ to the south-east of the main protocluster, hosting two prominent bow shocks visible in H_2 emission driven by at least two actively forming YSOs.

The content of this document has been adapted from the accepted publications in The Astrophysical Journal presented in Crowe et al. (2024a) and Bally et al. (2024).

1 Introduction

Massive stars ($m_* > 8 M_\odot$) are fundamental in star and planet formation, they impact their birthplaces from early on in their formation ionizing the interstellar medium through their radiation and winds. They also drive much of the physical and chemical evolution of galaxies as many of these massive protostars will end their life in the form of supernovae. However, formation mechanisms for massive stars are still poorly understood. In particular, it is unclear whether they form in a similar, but scaled-up, manner as low-mass stars, or whether they form more chaotically at the centre of dense clusters (see, e.g., Tan et al. 2014; Rosen et al. 2020, for reviews).

One of the most extreme star-forming environments in our Milky Way is the Central Molecular Zone (CMZ), usually defined as the region within a Galactocentric radius of ~ 300 pc (see, e.g., Henshaw et al. 2023). This is a region of high metallicity (i.e., about $2 \times Z_\odot$; Giveon et al. 2002; Schödel et al. 2020; Nogueras-Lara 2022), thermal pressures ($P_{\text{th}} \sim 10^{-10}$ erg cm $^{-3}$; Morris & Serabyn 1996), molecular gas temperatures (e.g., $\gtrsim 60$ K; Ginsburg et al. 2016), cosmic ray ionization rates ($\zeta \gtrsim 10^{-15}$ s $^{-1}$; Carlson et al. 2016), and magnetic field strengths ($\geq 50 \mu\text{G}$ over large scales and up to ~ 5 mG in dense molecular clouds; Pillai et al. 2015). In this extreme environment, there is an asymmetry of dense gas distribution (and therefore star formation) in the CMZ, with around 2/3 of the dense gas being located at positive (eastern) Galactic longitudes (Yusef-Zadeh et al. 2009; Sormani et al. 2018).

Sagittarius C (hereafter Sgr C) is an active star-forming region in the CMZ, and therefore one of the key laboratories for testing theories of star formation in this extreme environment (Yusef-Zadeh et al. 1984; Law & Yusef-Zadeh 2004; Kendrew et al. 2013; Lu et al. 2016, 2019b,a, 2022). SgrC is the most massive and luminous star-forming region in the western (negative longitude) side of the CMZ (Kendrew et al. 2013), and it holds large reserves of gas that are necessary to produce the observed star formation activity. In this region, much attention has been paid to the most luminous source in the cloud, G359.44–0.102 (Kendrew et al. 2013), and its immediate surroundings. The source itself is a prominent “Extended Green Object” (Cyganowski et al. 2008; Chen et al. 2013), a class of objects visualised in Spitzer-IRAC images (identified in the $4.5 \mu\text{m}$ IRAC2 filter) and associated with massive star formation, methanol maser emission and protostellar outflows. There has been some discussion if the rest of the Sgr C cloud is quiescent (e.g., Kendrew et al. 2013) or star-forming (e.g., Lu et al. 2016). From the analysis of ALMA Band 6 continuum data, Lu et al. (2020) and Kinman et al. (2024) have found > 100 low- to high-mass mm cores distributed throughout Sgr C, indicating that star formation is likely more widespread.

2 Main Results

The top panel of Figure 1 shows a Red(F480M) - Green(F360M) - Blue(F182M) image of Sgr C and its surroundings covering a total FOV of $2' \times 6'$. These filters mainly trace continuum

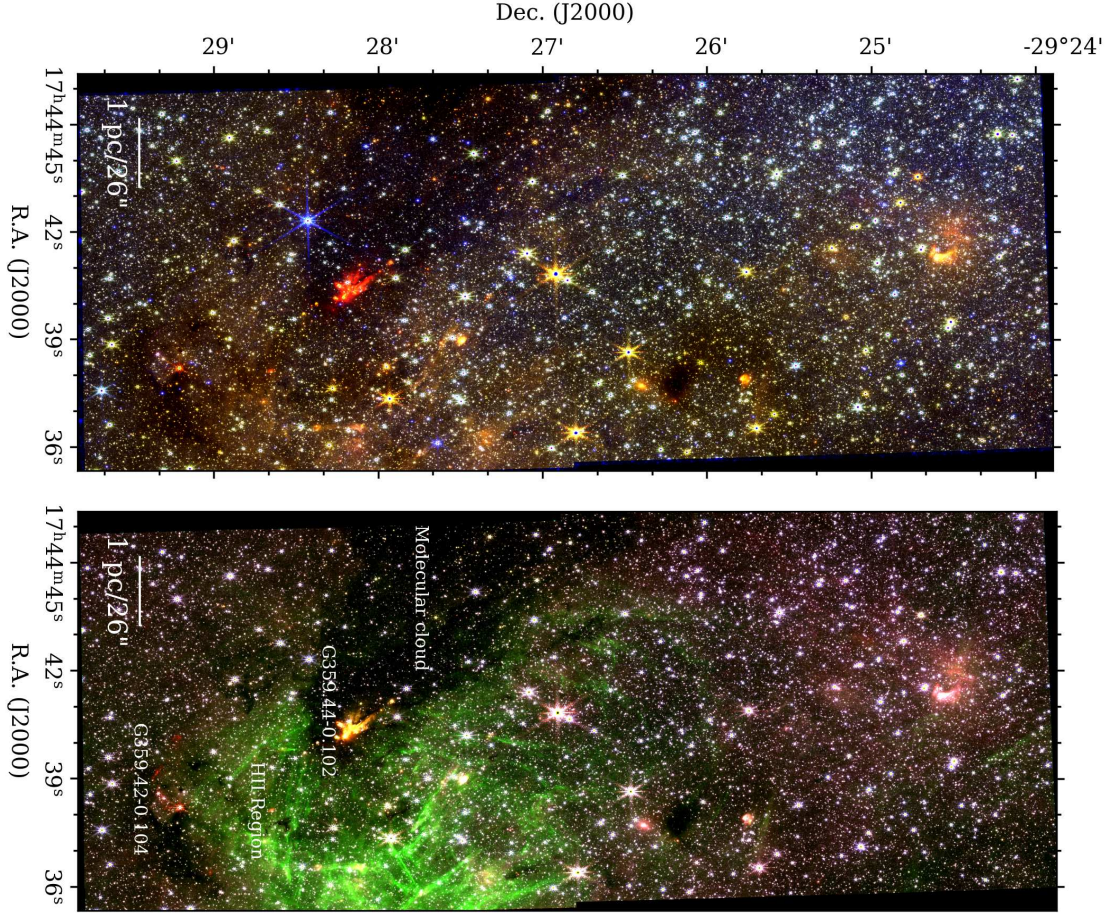


Figure 1: RGB image of Sgr C showing two different color schemes. N is right and E is up in both panels. *Top*: “Continuum” image with F480M shown in red, F360M in green, and F182M in blue. *Bottom*: “Emission line” image with F470N shown in red, F405N in green, and F360M in blue. Features of interest are labelled. Note that the figure is rotated 90 degrees with the y-axis R. A..

emission, especially from stars. The bright red emission to the south of the image is the primary target of the observation, the massive protostellar source G359.44-0.102 in Sgr C, and its associated protocluster. Engulfing this region there is a molecular cloud, which blocks much of the light from background stars. This cloud extends mainly to the east and north of the protocluster. The bottom panel of Figure 1 shows the same region, but now red is used for the F470N filter (H_2 0-0 S(9) line at $4.6947\,\mu\text{m}$), green for F405N (covering the Hydrogen Recombination Line -HRL- Br- α at $4.05\,\mu\text{m}$), and blue for F360M (mostly covers continuum at $3.6\,\mu\text{m}$). Most prominent in this image is the glow of HRL emission Br- α , which traces ionised gas surrounding G359.44-0.102 in northern, western and southern directions. The Br- α nebula displays remarkable linear, “needle”-like features, which have a variety of orientations, which may be related to large-scale magnetic fields (see Bally et al. 2024). This panel includes labels for the most prominent features in the region discussed above.

In the G359.44-0.102 star-forming region, there are two dominant massive protostars, G359.44a and G359.44b. Combining the JWST-NIRCam observations with ancillary data from the near- to the far-infrared from Spitzer, SOFIA, and Herschel, the main physical properties via SED-fitting have been derived (see Fedriani et al. 2023b, for details in the fitting). Both protostars have estimated protostellar masses of $\sim 20 M_{\odot}$ and bolometric luminosities $> 10^4 L_{\odot}$. Figure 2 shows a zooming view of the main massive star-forming region, with the JWST-NIRCam images of Br α and H $_2$ continuum-subtracted shown in green and red, respectively. These images reveal a plethora of outflow knots, 88 in total, with many of them associated with the two main protostars. This may indicate episodic accretion resulting in the ejection of outflow knots from the source, a phenomenon that has been previously observed in massive star-forming regions (e.g., Caratti o Garatti et al. 2017; Cesaroni et al. 2018; Fedriani et al. 2023a). The outflow axis as well as their outflow cavity walls are also very well-defined. In order to further peer into the larger scale star-forming region, we combined the IR data with sub-mm from ALMA to reveal and cross-match young stellar objects (YSOs) candidates, especially across the molecular cloud.

Finally, we also report the discovery of a new star-forming region revealed via H $_2$ line emission features indicating star formation activity $\sim 1'$ to the South of the main Sgr C protocluster. We name this star-forming region G359.42-0.104. It can be seen to the south of the bright HII region shown in Figure 1 bottom panel. The red channel in the RGB image, showing the F470N filter, i.e., shocked H $_2$ emission, reveals two prominent bow shocks.

3 Summary and conclusions

In this study (Crowe et al. 2024a), we have presented NIRCam observations of the CMZ star-forming region Sgr C which, along with ancillary IR and millimetre data, provide a high level of detail into the star formation activity of the main cloud and its surroundings. We have characterised the two most massive protostars in the heart of the main Sgr C protocluster, G359.44a and G359.44b, and obtained their physical properties via SED-fitting; in particular, masses of $\sim 20 M_{\odot}$ have been derived for each protostar. We have made a cross-match between JWST sources and ALMA cores in order to identify a sample of lower-mass protostars. From these sources, there are 5 matches that are redder than the overall population, which we take to be our strongest sample of low-mass YSOs in the cloud. We have carried out a census of the narrow-band NIRCam data, using the filters F212N, F405N, and F470N, which trace shocked molecular and atomic hydrogen emission from protostellar jets, to identify line-emitting features. We have identified 88 features, which we believe to comprise protostellar outflows from over a dozen protostellar outflows in the NIRCam data. We attribute about a quarter of these outflow knots to the massive protostars G359.44a and G359.44b, forming an outflow axis for each protostar that agrees well with molecular line data from ALMA and archival IR data from Spitzer. There are ~ 40 others likely originating from other, lower-mass star formation activity in the cloud.

The remaining outflow knots are attributed to a newly-discovered star-forming region, G359.42-0.104, located $\sim 1'$ to the South of the main Sgr C protocluster. NIRCam data in G359.42-0.104 reveals a pair of prominent bow shocks in both F470N and F212N (tracing H $_2$

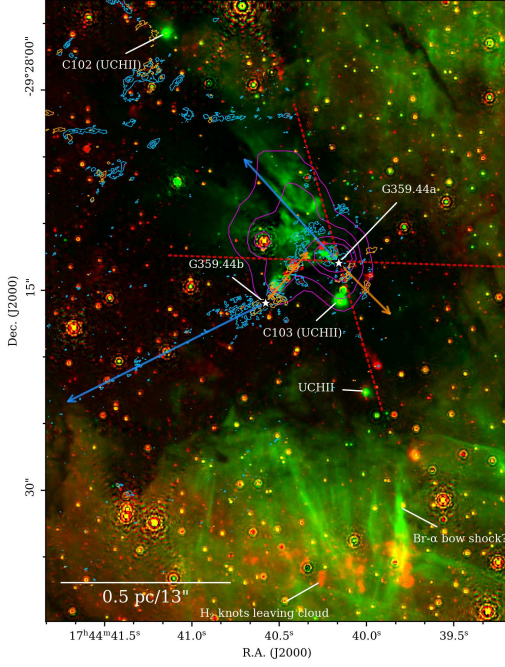


Figure 2: Central region of G359.44-0.102 with the two main massive protostars labelled as white star symbols, i.e. G359.44a and G359.44b. F470N is shown in red and F405N in green, both continuum-subtracted (see Crowe et al. 2024b, for methods). Blue and orange contours show ALMA Band 6 SiO 5-4 data from Lu et al. (2021) in blueshifted emission (integrated from -80 to -51 km s^{-1}) and redshifted emission (integrated from -48 to -25 km s^{-1}), respectively (similar to Figure 21 of Lu et al. 2021). The blue- and redshifted outflow axis of each source is indicated by the blue and orange arrows, respectively. Purple contours show Spitzer IRAC2 4.5 μm emission around G359.44a. The outflow cone of G359.44a measured from the NIRCcam data is indicated by the dotted red lines.

shocked emission), which we estimate to have originated from two protostars, G359.42a and G359.42b, the former of which we speculate may be a massive protostar due to its SED-fit inferred mass ($m_* > 8M_\odot$). However, the distance to this region, and whether it is inside the CMZ or foreground, is still uncertain.

Acknowledgments

S.T.C. acknowledges support from the award JWST-GO-04147.003-A. R.F. acknowledges support from the grants Juan de la Cierva FJC2021-046802-I, PID2020-114461GB-I00, and PID2023-146295NB-I00. R.F., L.B.F., and R.S. acknowledge financial support from the Severo Ochoa grant CEX2021-001131-S funded by MCIN/AEI/ 10.13039/501100011033. Additionally, L.B.F. and R.S. acknowledge support from grant EUR2022-134031 funded by MCIN/AEI/10.13039/501100011033 and by the European Union NextGenerationEU/PRTR. and grant PID2022-136640NB-C21 funded by MCIN/AEI 10.13039/501100011033 and by the European Union. Y.Z. acknowledges the support from the Yangyang Development Fund. Y.C. was partially supported by a Grant-in-Aid for Scientific Research (KAKENHI number JP24K17103) of the JSPS. J.B. acknowledges support by National Science Foundation through grant No. AST-1910393. A.G. acknowledges support from the NSF under grants AAG 2008101, 2206511, and CAREER 2142300. Y.-L.Y. acknowledges support from Grant-in-Aid from the Ministry of Education, Culture, Sports, Science, and Technology of Japan (20H05845, 20H05844), and a pioneering project in RIKEN (Evolution of Matter in the Universe). Z.-Y.L. is supported in part by NSF AST- 2307199 and NASA 80NSSC20K0533.

References

- Bally, J., Crowe, S., Fedriani, R., et al. 2024, arXiv e-prints, arXiv:2412.10983
- Caratti o Garatti, A., Stecklum, B., Garcia Lopez, R., et al. 2017, *Nature Physics*, 13, 276
- Carlson, E., Linden, T., & Profumo, S. 2016, *Phys. Rev. D*, 94, 063504
- Cesaroni, R., Moscadelli, L., Neri, R., et al. 2018, *A&A*, 612, A103
- Chen, X., Gan, C.-G., Ellingsen, S. P., et al. 2013, *ApJS*, 206, 9
- Crowe, S., Fedriani, R., Tan, J. C., et al. 2024a, arXiv e-prints, arXiv:2410.09253
- Crowe, S., Fedriani, R., Tan, J. C., et al. 2024b, *A&A*, 682, A2
- Cyganowski, C. J., Whitney, B. A., Holden, E., et al. 2008, *AJ*, 136, 2391
- Fedriani, R., Caratti o Garatti, A., Cesaroni, R., et al. 2023a, *A&A*, 676, A107
- Fedriani, R., Tan, J. C., Telkamp, Z., et al. 2023b, *ApJ*, 942, 7
- Ginsburg, A., Henkel, C., Ao, Y., et al. 2016, *A&A*, 586, A50
- Giveon, U., Sternberg, A., Lutz, D., Feuchtgruber, H., & Pauldrach, A. W. A. 2002, *ApJ*, 566, 880
- Henshaw, J. D., Barnes, A. T., Battersby, C., et al. 2023, in *Astronomical Society of the Pacific Conference Series*, Vol. 534, PPVII, ed. S. Inutsuka, Y. Aikawa, T. Muto, K. Tomida, & M. Tamura, 83
- Kendrew, S., Ginsburg, A., Johnston, K., et al. 2013, *ApJ*, 775, L50
- Kinman, A. V. I., Petkova, M. A., Tan, J. C., Cosentino, G., & Cheng, Y. 2024, arXiv e-prints, arXiv:2403.04032
- Law, C. & Yusef-Zadeh, F. 2004, *ApJ*, 611, 858
- Lu, X., Cheng, Y., Ginsburg, A., et al. 2020, *ApJ*, 894, L14
- Lu, X., Li, G.-X., Zhang, Q., & Lin, Y. 2022, *Nature Astronomy*, 6, 837
- Lu, X., Li, S., Ginsburg, A., et al. 2021, *ApJ*, 909, 177
- Lu, X., Mills, E. A. C., Ginsburg, A., et al. 2019a, *ApJS*, 244, 35
- Lu, X., Zhang, Q., Kauffmann, J., et al. 2019b, *ApJ*, 872, 171
- Lu, X., Zhang, Q., Kauffmann, J., et al. 2016, arXiv e-prints, arXiv:1609.08240
- Morris, M. & Serabyn, E. 1996, *ARA&A*, 34, 645
- Nogueras-Lara, F. 2022, *A&A*, 666, A72
- Pillai, T., Kauffmann, J., Tan, J. C., et al. 2015, *ApJ*, 799, 74
- Rosen, A. L., Offner, S. S. R., Sadavoy, S. I., et al. 2020, *Space Sci. Rev.*, 216, 62
- Schödel, R., Nogueras-Lara, F., Gallego-Cano, E., et al. 2020, *A&A*, 641, A102
- Sormani, M. C., Treß, R. G., Ridley, M., et al. 2018, *MNRAS*, 475, 2383
- Tan, J. C., Beltrán, M. T., Caselli, P., et al. 2014, in *PPVI*, ed. H. Beuther & et al., 149–172
- Yusef-Zadeh, F., Hewitt, J. W., Arendt, R. G., et al. 2009, *ApJ*, 702, 178
- Yusef-Zadeh, F., Morris, M., & Chance, D. 1984, *Nature*, 310, 557